PROCEEDINGS OF SCIENCE

Phase transitions and gravitational waves in models of $\mathbb{Z}_{\mathbb{N}}$ scalar dark matter

Nico Benincasa[∗a], **Kristjan Kannike**[a], **Andi Hektor**[a], **Andrzej Hryczuk**[bc] **and Kaius Loos**[a]

[a] *National Institute of Chemical Physics and Biophysics, Rävala 10, Tallinn, Estonia*

[b] *Department of Physics, University of Oslo, Box 1048, NO-0316 Oslo, Norway*

[c] *National Centre for Nuclear Research, Hoża 69, 00-681, Warsaw, Poland*

E-mail: nico.benincasa@kbfi.ee, Kristjan.Kannike@cern.ch, Andi.Hektor@cern.ch, andrzej.hryczuk@ncbj.gov.pl, kaius.loos@gmail.com

We study the nature of phase transitions and gravitational wave signals in models of scalar dark matter with $\mathbb{Z}_{\mathbb{N}}$ symmetries. The scalar sector comprises the Standard Model Higgs, an Inert Doublet and a complex singlet. In such models, the dark matter relic density can be largely determined by semi-annihilations instead of usual annihilations, which reduces the direct detection signal. We perform a thorough study of the parameter space, investigating the impact of the quartic semi-annihilation couplings on the structure of potential minima, phase transitions, and possible enhancements of the stochastic gravitational wave signal.

European Physical Society Conference on High Energy Physics - EPS-HEP2019 - 10-17 July, 2019 Ghent, Belgium

∗Speaker.

 https://pos.sissa.it/

PoS(EPS-HEP2019)089

1. Introduction

Dark matter is hypothetical matter that can account for several problems encountered in astrophysics such as galaxy rotation curves, or galaxy-cluster collisions. Thanks to the Planck mission, one knows that the energy content of the Universe consists of 26.8% of dark matter [1]. Despite this significant proportion, one still does not know what dark matter exactly is. So far, plenty dark matter models have been studied, putting constraints on it. In 2012, Higgs boson, an elementary scalar particle, was discovered in the LHC [2,3]. Therefore, dark matter might be composed of elementary scalar particles as well.

2. Motivations

The motivation to study such models is that for $N \geq 3$, semi-annihilation processes become possible. It especially leads to reduced direct detection signal. In addition, scalar dark matter is responsible of richer phase-transition patterns and it is well-known that first-order phase transitions generate gravitational waves [4–6]. The latter could be then probed by future space-based gravitational-wave detectors such as LISA or BBO [7,8].

3. Model

Scalar dark matter one considers in this paper is invariant under the $\mathbb{Z}_3$ group. The symmetry transformation for a field ϕ is $\phi \to \omega^X \phi$, with $\omega = e^{2\pi i/3}$ and $X \in \{0,1,2\}$. Given that the most general scalar potential, which contains semi-annihilations terms, one can construct is the following

$$\begin{aligned} V = {} & \mu_1^2|H_1|^2 + \lambda_1|H_1|^4 + \mu_2^2|H_2|^2 + \lambda_2|H_2|^4 + \mu_S^2|S|^2 + \lambda_S|S|^4 \\ & + \lambda_{S1}|S|^2|H_1|^2 + \lambda_{S2}|S|^2|H_2|^2 + \lambda_3|H_1|^2|H_2|^2 + \lambda_4(H_1^\dagger H_2)(H_2^\dagger H_1) \\ & + \frac{\mu_S''}{2}(S^3 + S^{\dagger 3}) + \frac{\lambda_{S12}}{2}(S^2 H_1^\dagger H_2 + S^{\dagger 2} H_2^\dagger H_1) + \frac{\mu_{SH}}{2}(S H_2^\dagger H_1 + S^\dagger H_1^\dagger H_2) \end{aligned} \tag{3.1}$$

where $H_1 \to H_1$ is the Standard-model Higgs doublet, $H_2 \to e^{2\pi i/3} H_2$ is an inert Higgs doublet and $S \to e^{2\pi i/3} S$ is a complex scalar singlet [9].

The μ_S'' and λ_{S12} terms are responsible for semi-annihilation processes. The μ_{SH} term in the potential (3.1) induces a mixing between the singlet S and the neutral (lower) part of the inert doublet H_2. Through a change of basis, one can express H_2 and S in terms of the mass eigenstates x_1 and x_2:

$$H_2 = \begin{pmatrix} -iH^\pm \\ x_1 \sin\theta + x_2 \cos\theta \end{pmatrix} \text{ and } S = x_1 \cos\theta - x_2 \sin\theta \tag{3.2}$$

with θ the mixing angle.

Regarding the Standard model Higgs doublet, one writes it as usual in the unitary gauge: $H_1 = \begin{pmatrix} 0 \\ v+h \end{pmatrix}$, with $v \simeq 246$ GeV, its vacuum expectation value and h the Higgs boson. Without loss of generality, one considers the mass of x_1 lower than the mass of x_2, which implies that x_1 is the dark matter candidate. Then, taking θ such that $0 \leq \theta \leq 0.06$ ensures that the dark-matter candidate x_1 is dominantly singlet-like so that one does not measure a too large direct detection rate [9].

4. Constraints

In this section, one reviews a series of constraints that are applied to the model described in the previous section:

- unitarity: this constraint come from the unitarity of the scattering matrix. It results in $|\mathrm{Re}\ a_0^i| \leq 1/2$, $\forall i$, where a_0 is the zero order partial wave amplitude and the a_0^i its eigenvalues. Only quartic couplings are constrained from considering scattering in the infinite energy limit, while the dimensionful parameters such as $\mu_S^{''}$ are constrained by the unitarity of finite energy scattering.
- perturbativity: following Lerner and McDonald paper [10], one obtains

$$|\lambda_1| < \frac{2\pi}{3},\ |\lambda_2| < \pi,\ |\lambda_3| < 4\pi,\ |\lambda_4| < 4\sqrt{2}\pi,\ |\lambda_3 + \lambda_4| < 4\pi,$$
$$|\lambda_S| < \pi,\ |\lambda_{S1}| < 4\pi,\ |\lambda_{S2}| < 4\pi,\ |\lambda_{S12}| < 4\pi \tag{4.1}$$

- vacuum stability: the potential (3.1) has to be bounded below, especially in the limit of large field values, so that it presents a finite minimum. Only the quartic terms are relevant in this limit, which means that the vacuum stability constraint uniquely applies on the λ_i terms. By applying the procedure given in [11], one guarantees a quartic potential that is bounded below.
- globality of the vacuum: one requires that the electroweak symmetry breaking vacuum ($\langle S \rangle = \langle H_2 \rangle = 0$, with $\langle\ \rangle$ representing the vacuum expectation value of a field) to be the global minimum of the potential.
- dark-matter relic density: given Planck data, one knows that the dark-matter relic density has to satisfy $\Omega_{\mathrm{DM}} h^2 = 0.12 \pm 0.001$ [1].
- Higgs invisible branching ratio: in the situation where one has $2M_{x_1} \leq M_h \simeq 125$ GeV, the Higgs boson can decay into dark-matter particles, which results in a invisible decay. One defines the Higgs invisible branching ratio as

$$\mathrm{BR}_{\mathrm{inv}} = \frac{\Gamma^{\mathbb{Z}_3}_{h\to x_1 x_1^*}}{\Gamma^{\mathbb{Z}_3}_{h\to x_1 x_1^*} + \Gamma^{\mathrm{SM}}_h} \tag{4.2}$$

  with Γ_h^{SM}, the Higgs total decay width in the Standard Model.

  One must have $\mathrm{BR}_{\mathrm{inv}} < 0.24$ at 95% confidence level [12].
- electroweak precision tests: the constraint on the T parameter basically imposes $|M_{H^\pm} - M_{x_2}| \lesssim 120$ GeV on the mass splitting of $H^\pm$ with the doublet-like neutral scalar x_2 [9].
- LEP limits: the Large Electron Positron collider imposes $M_{H^\pm} > 80$ GeV [13].

5. Dark-matter relic density

The main processes that contribute to dark-matter relic density, are due to three terms in the potential (3.1). First, annihilation is governed by the λ_{S1} term. For instance, one can have two diagrams where in the first one, dark-matter particles annihilate into Higgs bosons and in the second one they annihilate into Standard model particles.

As for semi-annihilation, when the mixing angle θ is small, it depends on μ_S'' and/or λ_{S12}. On the one hand, $x_1 x_1^* \to x_1 \to h x_1^*$ contributes more for relatively light dark-matter masses, when $M_{x_1} > M_h$. On the other hand, other semi-annihilation processes like $x_1 x_1^* \to h x_2$ can dominate. This is the case when $M_{x_2} + M_h < 2M_{x_1}$. Semi-annihilation becomes important when the value of μ_S'' and/or λ_{S12} is large. To conclude, coannihilation is allowed when the difference between M_{x_1}, M_{x_2} and/or $M_{H^\pm}$ is small. As an example of these new semi-annihilation processes, one has $x_1 x_2 \to x_1 Z,\ x_1 h$ or $x_1 H^+ \to x_1 W^+$.

6. Results

Regarding the parameter space, we take $M_{x_1} \in [10, 1000]$ GeV and $M_{x_2}, M_{H^\pm} \in [M_{x_1} + 0.01, 4000]$ GeV. Next, we consider $\mu_S'' = 0$ and $|\lambda_{S12}| \in [0, 2\pi]$. We fit λ_{S1} to the dark-matter relic density. As for, $\lambda_2, \lambda_3, \lambda_4$ and λ_S, they are free and are varied from 0 to π to make the potential bounded from below (vacuum stability). We do not take the full range allowed by unitarity and perturbativity but some more reasonable upper bound.[1] Finally, to calculate relic density and direct detection, we use micrOMEGAs [14] and to compute gravitational waves we use CosmoTransitions [15] and the non-runaway scenario described in [16].

6.1 Direct detection

We present the direct detection results in Fig. 1 where the colour code characterises the fraction of semi-annihilation α, which is equal to 1 if there are only semi-annihilation processes and is equal to 0 if there is no semi-annihilation. We see that scenarios with large semi-annihilation lead to suppressed direct detection rate. Furthermore, we can observe that several points with a low α yield a smaller direct detection rate. These points are due to coannihilation processes. Indeed, if coannihilation is dominant, then annihilation (and thus the direct detection cross section) has to be smaller to obtain the right relic density. Next, we can see in the left part of the scatter plot that there is no point anymore below $M_{x_1} \simeq 55$ GeV. This is explained by the Higgs invisible branching ration constraint. As a final note, we see that with XENONnT [17], only a few point could escape this detector, therefore the model could be nearly completely tested.

6.2 Gravitational wave

Fig. 2 shows gravitational wave signals. The signals we obtain only come from phase transitions that also exist in the inert doublet model or two-Higgs doublet model. There is

[1] We take the maximal values at a fraction of the perturbativity bound and not right at its upper bound, so that we do not hit the Landau pole of the scalar couplings at once.

PoS(EPS-HEP2019)089

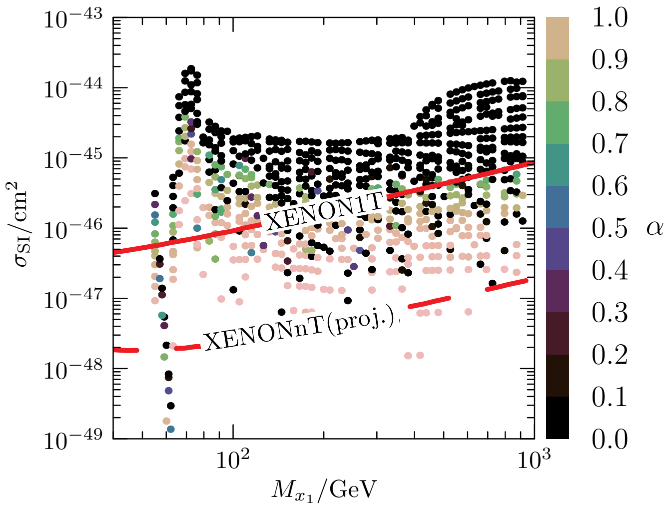

Figure 1: Dark-matter spin-independent direct detection cross section σ_{SI} as a function of the dark-matter mass M_{x_1}. The colour code shows the fraction of semi-annihilation α. The solid line is the exclusion limit for XENON1T at 90% C.L. [18], whereas the dashed line is the projected exclusion limit for XENONnT.

no new contribution[2] to the two aforementioned models due to the presence of the singlet S, thereby there is no phase transition that would involve a phase with $\langle H_1 \rangle$, $\langle H_2 \rangle$ and $\langle S \rangle$ all non-zero. If it were the case, then the quartic semi-annihilation coupling λ_{S12} would also be involved. A possible explanation for this missing case is that a minimum involving λ_{S12} is generally deeper than minima with only $\langle H_1 \rangle \neq 0$, which means that the global minimum would be with $\langle S \rangle \neq 0$ so it would break the $\mathbb{Z}_3$ symmetry of the model.

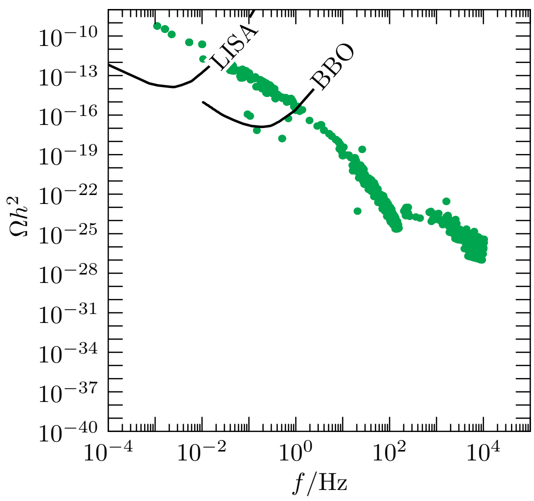

Figure 2: Scatter plot of the peak power Ωh^2 of gravitational waves signals as a function of the frequency f. The two curves represent the sensitivity of LISA and BBO experiments.

[2]Of course, some transitions with the singlet are possible like $(0,0,0) \to (0,0,v_S) \to (v_1,0,0)$, with $\langle S \rangle = v_S$ and $\langle H_1 \rangle = v_1$, for instance.

7. Conclusion

The semi-annihilation feature of the $\mathbb{Z}_3$ model is responsible for suppressed direct detection cross section and first-order phase transitions can give a potentially detectable stochastic gravitational wave signals.

References

[1] Planck collaboration, *Planck 2018 results. VI. Cosmological parameters*, 1807.06209.

[2] ATLAS collaboration, *Observation of a new particle in the search for the Standard Model Higgs boson with the ATLAS detector at the LHC*, *Phys. Lett.* **B716** (2012) 1 [1207.7214].

[3] CMS collaboration, *Observation of a New Boson at a Mass of 125 GeV with the CMS Experiment at the LHC*, *Phys. Lett.* **B716** (2012) 30 [1207.7235].

[4] P. J. Steinhardt, *Relativistic Detonation Waves and Bubble Growth in False Vacuum Decay*, *Phys. Rev.* **D25** (1982) 2074.

[5] C. J. Hogan, *NUCLEATION OF COSMOLOGICAL PHASE TRANSITIONS*, *Phys. Lett.* **133B** (1983) 172.

[6] E. Witten, *Cosmic separation of phases*, *Phys. Rev. D* **30** (1984) 272.

[7] eLISA collaboration, *The Gravitational Universe*, 1305.5720.

[8] V. Corbin and N. J. Cornish, *Detecting the cosmic gravitational wave background with the big bang observer*, *Class. Quant. Grav.* **23** (2006) 2435 [gr-qc/0512039].

[9] G. Bélanger, K. Kannike, A. Pukhov and M. Raidal, *Minimal semi-annihilating $\mathbb{Z}_N$ scalar dark matter*, *JCAP* **1406** (2014) 021 [1403.4960].

[10] R. N. Lerner and J. McDonald, *Gauge singlet scalar as inflaton and thermal relic dark matter*, *Phys. Rev.* **D80** (2009) 123507 [0909.0520].

[11] K. Kannike, *Vacuum Stability of a General Scalar Potential of a Few Fields*, *Eur. Phys. J.* **C76** (2016) 324 [1603.02680].

[12] CMS collaboration, *Searches for invisible decays of the Higgs boson in pp collisions at $\sqrt{s}$ = 7, 8, and 13 TeV*, *JHEP* **02** (2017) 135 [1610.09218].

[13] A. Pierce and J. Thaler, *Natural Dark Matter from an Unnatural Higgs Boson and New Colored Particles at the TeV Scale*, *JHEP* **08** (2007) 026 [hep-ph/0703056].

[14] G. Bélanger, F. Boudjema, A. Goudelis, A. Pukhov and B. Zaldivar, *micrOMEGAs5.0 : Freeze-in*, *Comput. Phys. Commun.* **231** (2018) 173 [1801.03509].

[15] C. L. Wainwright, *CosmoTransitions: Computing Cosmological Phase Transition Temperatures and Bubble Profiles with Multiple Fields*, *Comput. Phys. Commun.* **183** (2012) 2006 [1109.4189].

[16] C. Caprini et al., *Science with the space-based interferometer eLISA. II: Gravitational waves from cosmological phase transitions*, *JCAP* **1604** (2016) 001 [1512.06239].

[17] XENON collaboration, *The XENON1T Dark Matter Experiment*, *Eur. Phys. J.* **C77** (2017) 881 [1708.07051].

[18] XENON collaboration, *Dark Matter Search Results from a One Ton-Year Exposure of XENON1T*, *Phys. Rev. Lett.* **121** (2018) 111302 [1805.12562].

PoS(EPS-HEP2019)089